Supplementary Information

Density color map

The density color map used in Fig.1 is defined using a normalized distance function

$$R_{ij} = \sqrt{\left[\frac{(v_i - v_j)}{R_v}\right]^2 + \left[\frac{(CR_i - CR_j)}{R_{cr}}\right]^2}$$

where v_i and v_j are the final (noninteger) vibrational quantum numbers as obtained by the WKB procedure for trajectories i and j, CR_i and CR_j are corresponding CR values, and R_v and R_{cr} are two empirical normalizing values. R_v is set to 0.5 because it is the bin half-width, while R_{cr} is ¼ because the typical effects are seen over this scale of collision remoteness. (R_v and $R_{cr,}$, like v and $CR,$ are dimensionless). The color of the point associated with trajectory i follows a linear scale of density, defined by counting the number of other trajectories satisfying $R_{ij} < 1$ (that is, "in the neighborhood" of point i.) The density is then normalized to its maximum value in each panel to make comparisons easy.

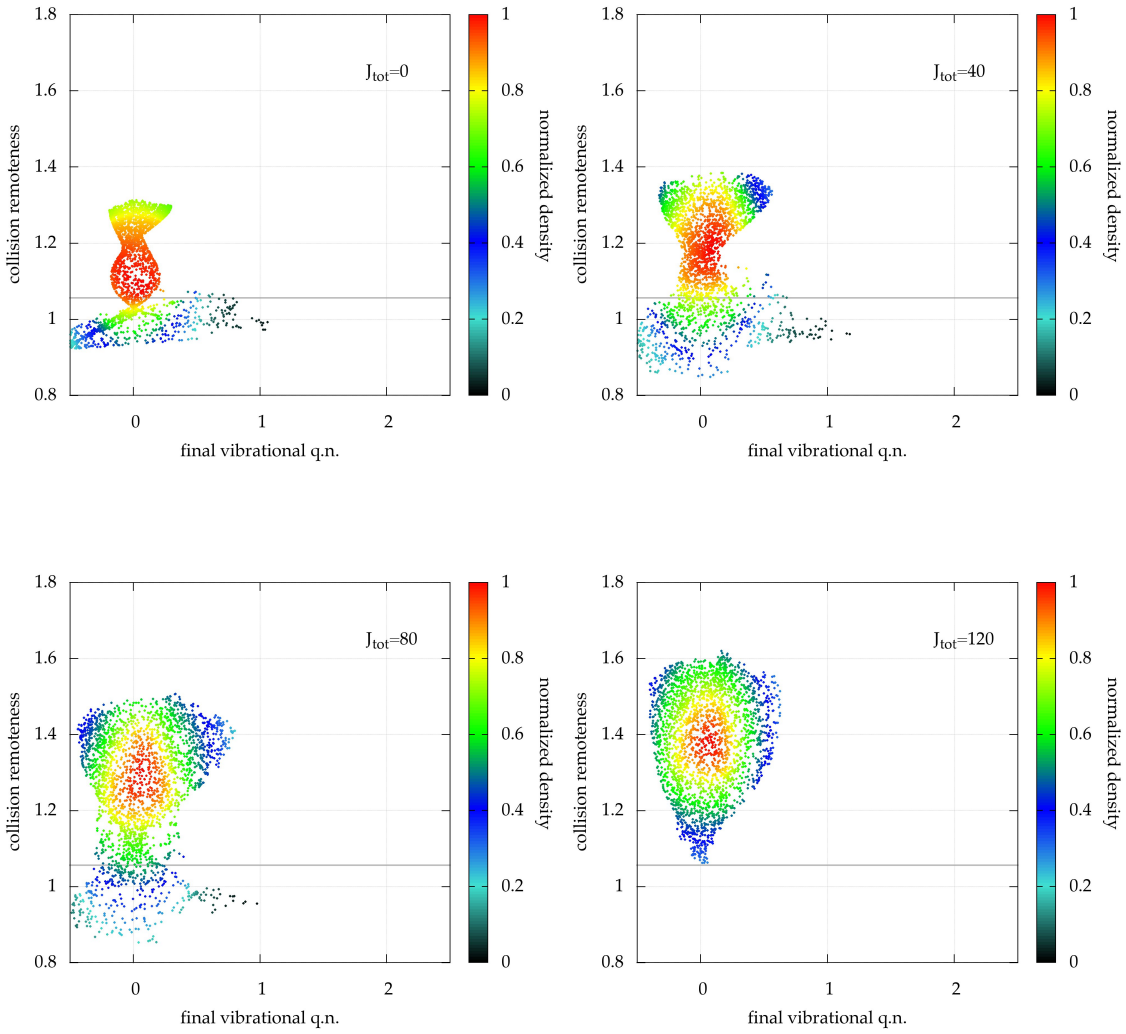

Figure S1

Same as for Figure 1, but considering a fixed collision energy of 3eV, varying J as indicated in the panels. For sufficiently high J, only PNR trajectories are found. QCT treats PNR trajectories roughly and QR trajectories with accuracy, while semiclassical methods used for vibrational energy transfer have been designed fundamentally thinking of PNR kind of collision. Collision remoteness discrimination can be the basis for different, complementary treatments.

Figure S1 shows the PNR and QR distributions as J is increased, at a fixed collision energy of 3 eV. At low J, the interaction is strong and both QR and PNR distributions are important. It is worth noting that the only contribution to the $v\prime = 1$ vibrational energy transfer at $J = 0$ is given exclusively by QR events; no PNR trajectory is found in that final bin using conventional $0.5 \leq v \leq 1.5$ limits, and with Gaussian binning [1] the condition would be even more stringent.

For higher J values, a few PNR trajectories can be found just at the lower limit of $v\prime = 1$ bin, but as well known, QCT results obtained only from trajectories at the bin borderline are of very poor quality [2, 3].

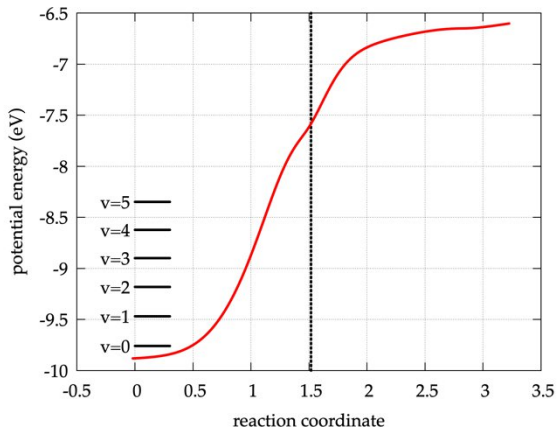

Figure S2.
MEP representation as a function of reaction coordinate. A small barrier (partially visible) is present at the right extremum of the interval considered. The vertical dotted line indicates the point of intersection with the QR diagonal. The region around this point is what in the text is indicated as SCR (at variance with barrier region). The first six vibrational levels are indicated.

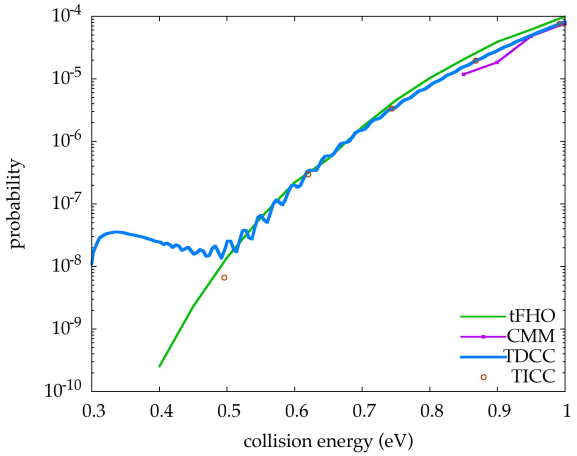

Figure S3
Comparison of tFHO, CMM, TDCC and TICC at low energy and very low probabilities. While CMM would require an unreasonable trajectory number for so low probabilities, tFHO appears perfectly able to reproduce with accuracy the TICC result. In contrast, the TDCC method appears to be limited to probability values above 10^{-8} when using the wavepacket employed in the present calculations (see Methods section).

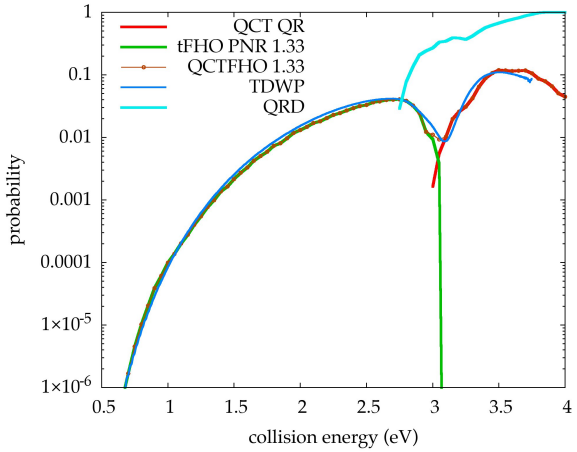

Figure S4

Comparison of TDWP probability with QCTFHO result obtained using a QR limit empirical value of 1.33 (instead of the original value of 1.055). QR limit for QCT-QR is the original one.

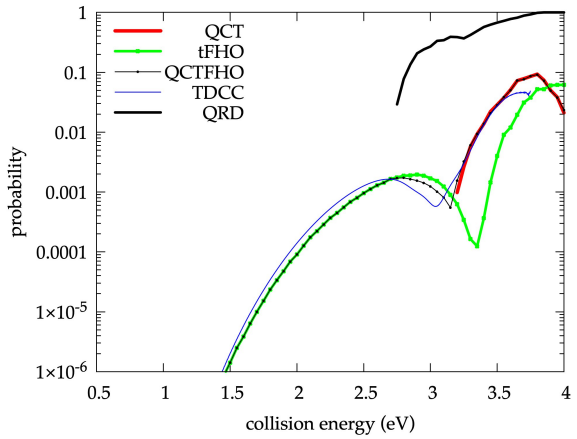

Figure S5

Same as in Figure 4, but for final vibration v'=2. Even in this case the agreement with accurate QM calculations is very good for QCTFHO result, but not for standard trajectory-based methods.

In Figure S5 a comparison is shown of QCT, tFHO, QCTFHO and TDCC in the same conditions as the Figure 4 but for final vibration $v' = 2$. The general observation is that what has been observed for $v' = 1$ is confirmed in this case, including the quite good general agreement with TDCC. In this case even pure tFHO appears slightly higher than TDCC in the QR region up to about 3eV. After that limit, it appears totally out of convergence, with a trend similar to TDCC but shifted towards higher collision energy values, as previously noted in the case $v' = 1$. QCT is almost coincident with TDCC up to 3.6eV, but shows no result for energy values lower than about 3.1eV. In this case, the low energy part seen in Figure 4 for $v' = 1$, peaked around 2.5eV and completely unreliable, is absent. This is a feature typical of a higher vibrational gap: QCT tends to be better in this case, in the sense that the non-zero result comes essentially from QCT-QR contribution and is realistic, often accurate. The zero result, on the contrary, comes from the absence of a QCT-PNR contribution, due to the higher vibrational gap; the transition is more classically forbidden [4]. This feature will be confirmed in the cross section results section. Even in this case, a direct application of the original methods QCT and tFHO would not provide an accurate result over the whole energy range.

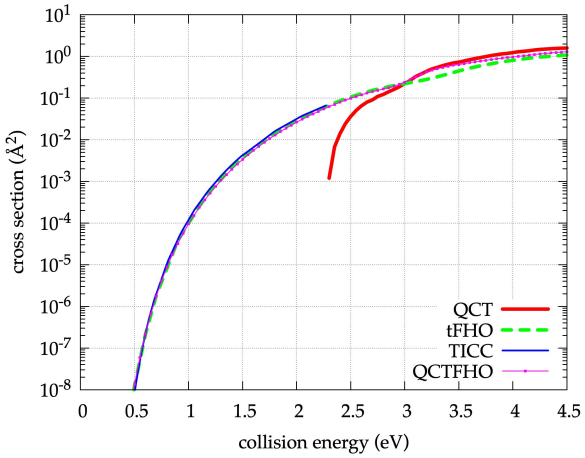

Figure S6
As for Figure 9, but considering v'=1,j'≤64. Even considering lower and higher final rotation, the tFHO and QCTFHO level of agreement does not degrade appreciably on the whole common collision energy range.

The excellent agreement with the TICC result seen in Figure 9 persists in Figure S6 where the cross section is summed over many higher and lower rotational final states, both for standard methods and QCTFHO. The hybrid method strictly follows tFHO up to 3eV, then follows QCT up to 3.5eV, and finally shows an intermediate trend between QCT and tFHO. This complex behavior is essentially confirmed also in the $v' = 2$ case in Figure S7. This abrupt passage from tFHO at low energy to QCT at high energy is not typical, as shown in Figures 10-12 when the collision starts from higher vibrational states. In general, the passage is smooth, with the two contributions simultaneously present in the cross section. This blending occurs because QR events are more likely at lower *J*, while the PNR contribution increases at high *J*, as discussed in relation to Figure 1.

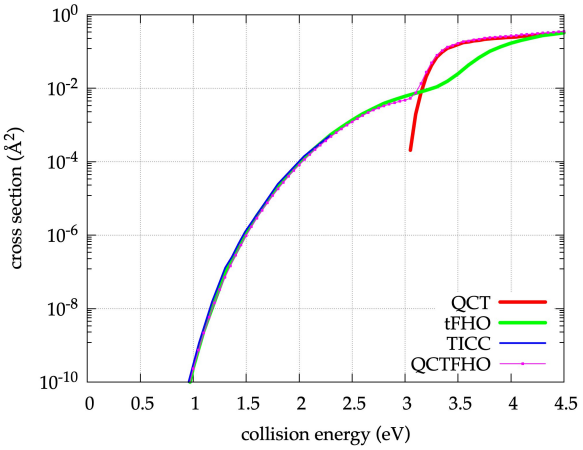

Figure S7
As for Figure 9, but with v'=2,j'≤64. When vibrational gap increases in the transition, QCTFHO tends to follow tFHO at low energy and QCT at high energy.

Supplementary Information References

1. Bonnet, L., Rayez, J.-C.: Gaussian weighting in the quasiclassical trajectory method. Chem. Phys. Lett. 397, 106–109 (2004). https://doi.org/10.1016/j.cplett.2004.08.068
2. Esposito, F.: Reactivity, relaxation and dissociation of vibrationally excited molecules in low-temperature plasma modeling. Rendiconti Lincei Sci. Fis. E Nat. 30, 57–66 (2019). https://doi.org/10.1007/s12210-019-00778-9
3. Mandy, M., Martin, P.: Integral cross sections for atomic hydrogen+ hydrogen (0, 0) -> hydrogen (0, j')+ hydrogen atom: comparison of quasiclassical and quantum results. J. Phys. Chem. 95, 8726–8731 (1991)
4. Miller, W.H.: Classical S Matrix: Numerical Application to Inelastic Collisions. J. Chem. Phys. 53, 3578 (1970). https://doi.org/10.1063/1.1674535